

# Nuclear transition matrix elements for Majoron-accompanied neutrinoless double- $\beta$ decay within a projected-Hartree-Fock-Bogoliubov model

P. K. Rath,<sup>1</sup> R. Chandra,<sup>2,\*</sup> K. Chaturvedi,<sup>3</sup> P. Lohani,<sup>1</sup> and P. K. Raina<sup>4</sup>

<sup>1</sup>Department of Physics, University of Lucknow, Lucknow 226007, India

<sup>2</sup>Department of Applied Physics, Babasaheb Bhimrao Ambedkar University, Lucknow 226025, India

<sup>3</sup>Department of Physics, Bundelkhand University, Jhansi 284128, India

<sup>4</sup>Department of Physics, Indian Institute of Technology, Ropar, Rupnagar 140001, India

(Received 29 January 2015; revised manuscript received 14 December 2015; published 16 February 2016)

The model-dependent uncertainties in the nuclear transition matrix elements for the Majoron-accompanied neutrinoless double- $\beta$  decay ( $0^+ \rightarrow 0^+$  transition) of  $^{94,96}\text{Zr}$ ,  $^{100}\text{Mo}$ ,  $^{128,130}\text{Te}$ , and  $^{150}\text{Nd}$  isotopes are calculated by employing the projected-Hartree-Fock-Bogoliubov formalism with four different parametrizations of the pairing plus multipolar two-body interactions and three different parametrizations of the Jastrow short-range correlations. Uncertainties in the nuclear transition matrix elements turn out to be less than 15% and 21% for decays involving the emission of single and double Majorons, respectively.

DOI: [10.1103/PhysRevC.93.024314](https://doi.org/10.1103/PhysRevC.93.024314)

## I. INTRODUCTION

A new generation of experiments searching for the neutrinoless double- $\beta$  ( $\beta\beta\phi$ )<sub>0ν</sub> decay is now running or being commissioned, which would be able to measure half-lives approaching  $10^{27}$  yr (see, for example, Refs. [1–3] and references therein). These will provide lower limits on the effective Majorana neutrino mass and more stringent limits on the effective parameters of gauge theoretical models beyond the standard model of electroweak unification. Within these models, several alternative mechanisms violating the conservation of lepton number  $L$  have been proposed, which could be observed in the  $(\beta\beta\phi)_0\nu$  decay [4]. The Majoron-accompanied neutrinoless double decay  $(\beta\beta\chi)_0\nu$  is one such possibility [5].

The proposed nine Majoron models can be broadly classified into classical [6–9] and new Majoron models [10–12], which may be alternatively distinguished as single Majoron emitting  $(\beta\beta\phi)_0\nu$  decay and double Majoron emitting  $(\beta\beta\phi\phi)_0\nu$  decay modes. However, the Gelmini-Roncadelli model [7] and the doublet Majoron model of Aulakh and Mohapatra [9] were inconsistent with the measured width of  $Z^0$  and ruled out [13,14]. Over the past decades, a series of experimental studies were performed, which provided limits on the Majoron coupling constant  $\langle g \rangle$  of the order of  $10^{-5}$  and information on the sensitivities of the ongoing experiments to different new Majoron models. The experimental aspects of the  $(\beta\beta\chi)_0\nu$  decay have been recently reviewed by Barabash [15] and references therein. Further, the observability of nine Majoron models have also been studied theoretically by Hirsch *et al.* [16] by employing the quasiparticle random-phase approximation (QRPA) approach.

To relate the experimental results with limits on Majoron-neutrino couplings, the evaluation of reliable nuclear transition matrix elements (NTMEs) is needed. Two main ingredients are required for this purpose: the wave functions of the initial and final nuclei and the translation of transition operators from the fundamental quark level to effective operators

at the nucleon level. The latter involves the inclusion of the finite size of nucleons (FNS), short-range correlations (SRC) [17–21] the, and choice of an effective value of the axial vector current coupling constant  $g_A$  [22–25]. The nuclear wave functions are calculated employing a variety of nuclear models, namely, shell model [26–28], QRPA [29,30] and its extensions [31,32], deformed QRPA [33,34], QRPA with isospin restoration [35], projected-Hartree-Fock-Bogoliubov (PHFB) [36–39], interacting boson model (IBM) [40,41] with isospin restoration [25], energy density functional (EDF) [42], and beyond-mean-field covariant density functional (BMF-CDFT) [43] approaches. Although, the Hilbert spaces and residual interactions are employed in quite different ways in each of them, it is remarkable that the resulting NTMEs  $M^{(0\nu)}$  differ only by a factor of 2–3.

The main proposals to estimate the uncertainties in NTMEs for the  $(\beta^-\beta^-)_0\nu$  decay are a model-independent comparison of the ratios of the NTMEs squared with the ratios of observed half-lives  $T_{1/2}^{(0\nu)}$  [44], treating the spread of the calculated NTMEs in different models [45] as the measure of the theoretical uncertainty [46,47], and a statistical analysis of model-specific theoretical uncertainties in the calculated NTMEs within the QRPA approach [48,49]. Further, uncertainties in NTMEs due to the SRC have also been investigated [20,21,50]. It has been recently observed by Engel [51] that, despite useful statistical analysis, large systematic errors inhibit, for the most part, a kind of careful error analysis advocated in Ref. [52]. By including all physics known to be important as emphasized by one or the other of the existing approaches, the systematic errors can be reduced.

The study of uncertainties in the NTMEs, calculated with the PHFB approach using four different parametrizations of a Hamiltonian and three different short-range correlations, was first performed for the  $(\beta^-\beta^-)_0\nu$  decay within the light Majorana neutrino mass mechanism [37]. Including higher-order currents (HOC), it was extended later for estimating uncertainties in the NTMEs, calculated for the exchange of light [38] and heavy Majorana neutrinos [39], the  $(\beta^+\beta^+)_{0\nu}$  decay [53], and the  $(\beta^-\beta^-)_{0\nu}$  decay involving classical

\*Corresponding author: rameshchandra@bbau.ac.in

Majorons and sterile neutrinos [38]. In Ref. [38], no difference has been observed in the effects due to the FNS either by employing dipole form factors or form factors taking the structure of nucleons into account.

The present work is an extension of estimating uncertainties in NTMEs for the  $(\beta^- \beta^- \chi)_{0\nu}$  decay modes within mechanisms involving new Majoron models. Results are presented for  $^{94,96}\text{Zr}$ ,  $^{100}\text{Mo}$ ,  $^{128,130}\text{Te}$ , and  $^{150}\text{Nd}$  isotopes, calculated within the PHFB approach by employing four different parametrizations of pairing plus multipolar effective two-body interaction, dipole form factor, and three different parametrizations of Jastrow SRC. The effects due to the FNS as well as the SRC vis-à-vis the radial evolution of NTMEs and deformation are also investigated.

## II. THEORETICAL FRAMEWORK

The detailed theoretical formalism to calculate the half-lives of the  $(\beta^- \beta^- \chi)_{0\nu}$  decay modes in nine Majoron models [12] have been discussed by Hirsch *et al.* [16]. Hence, an outline of the required theoretical formalism is given in the following for the clarity in notations used in the present work. The inverse half-life  $T_{1/2}^{(0\nu\chi)}$  for the  $0^+ \rightarrow 0^+$  transition of  $(\beta^- \beta^- \chi)_{0\nu}$  decay is given by

$$[T_{1/2}^{(0\nu\chi)}(0^+ \rightarrow 0^+)]^{-1} = |\langle g_\alpha \rangle|^m G_\alpha^{(\chi)} |M_\alpha^{(\chi)}|^2. \quad (1)$$

The index  $\alpha$  indicates the effective coupling constants  $g_\alpha$ , phase-space factors  $G_\alpha^{(\chi)}$ , and NTMEs  $M_\alpha^{(\chi)}$  for different Majoron models. The index  $m$  takes values 2 and 4 for the  $(\beta^- \beta^- \phi)_{0\nu}$  and  $(\beta^- \beta^- \phi\phi)_{0\nu}$  decay modes, respectively. The symbol  $\chi$  denotes modes involving a single Majoron,  $\phi$ , or two Majorons,  $\phi\phi$ . The phase-space factors are calculated using

$$G_\alpha^{(\chi)} = a_\alpha^{(\chi)} \int_1^{T+1} F_0(Z_f, \varepsilon_1) p_1 \varepsilon_1 d\varepsilon_1 \times \int_1^{T+2-\varepsilon_1} (T + 2 - \varepsilon_1 - \varepsilon_2)^n F_0(Z_f, \varepsilon_2) p_2 \varepsilon_2 d\varepsilon_2. \quad (2)$$

In Table I, we present the prefactors  $a_\alpha^{(\chi)}$  and NTMEs  $M_\alpha^{(\chi)}$  corresponding to different Majoron models.

TABLE I. Different Majoron models according to Bamert *et al.* [12].

Modes	Case	$n$	Prefactors $a_\alpha$	NTME
$\beta\beta\phi$	IB, IC, IIB	1	$\frac{2(G_F g_A)^4 m_e^9}{256\pi^7 \ln(2) (m_e R)^2}$	$M_{m_v}^{(\chi)}$
$\beta\beta\phi$	IIC, IIF	3	$\frac{2(G_F g_A)^4 m_e^9}{64\pi^7 \ln(2) (m_e R)^2}$	$M_{CR}^{(\chi)}$
$\beta\beta\phi\phi$	ID, IE, IID	3	$\frac{2(G_F g_A)^4 m_e^9}{12288\pi^9 \ln(2) (m_e R)^2}$	$M_{\omega^2}^{(\chi)}$
$\beta\beta\phi\phi$	IIE	7	$\frac{2(G_F g_A)^4 m_e^9}{215040 \pi^9 \ln(2) (m_e R)^2}$	$M_{\omega^2}^{(\chi)}$

In the closure approximation, the NTMEs  $M_\alpha^{(\chi)}$  are defined as

$$M_{m_v}^{(\chi)} = \sum_{n,m} \left\langle 0_F^+ \left| \left[ -\frac{H_F(r_{nm})}{g_A^2} + \boldsymbol{\sigma}_n \cdot \boldsymbol{\sigma}_m H_{GT}(r_{nm}) + S_{nm} H_T(r_{nm}) \right] \tau_n^+ \tau_m^+ \right| 0_I^+ \right\rangle, \quad (3)$$

$$M_{CR}^{(\chi)} = \left( \frac{g_V}{g_A} \right) \left( \frac{f_W}{3} \right) \sum_{n,m} \left\langle 0_F^+ \left| \boldsymbol{\sigma}_n \cdot \boldsymbol{\sigma}_m H_R(r, \bar{A}) \tau_n^+ \tau_m^+ \right| 0_I^+ \right\rangle, \quad (4)$$

$$M_{\omega^2}^{(\chi)} = \sum_{n,m} \left\langle 0_F^+ \left| \left( \frac{g_V}{g_A} \right)^2 - \boldsymbol{\sigma}_n \cdot \boldsymbol{\sigma}_m \right| H_{\omega^2}(r, \bar{A}) \tau_n^+ \tau_m^+ \right| 0_I^+ \right\rangle. \quad (5)$$

The NTMEs  $M_{m_v}^{(\chi)}$  of the classical Majoron models are the same as the NTMEs  $M^{(0\nu)}$  of the light Majorana neutrino mass mechanism and have been calculated in Ref. [38]. The neutrino potentials  $H_R(r, \bar{A})$  and  $H_{\omega^2}(r, \bar{A})$  required for the calculation of the other two matrix elements  $M_{CR}^{(\chi)}$  and  $M_{\omega^2}^{(\chi)}$ , respectively, are defined as

$$H_R(r, \bar{A}) = \frac{1}{4\pi^2 M} \int e^{iqr} \left[ \frac{\bar{A} + 2q}{q(q + \bar{A})^2} \right] \left( \frac{\Lambda^2}{q^2 + \Lambda^2} \right)^4 d^3 q, \quad (6)$$

$$H_{\omega^2}(r, \bar{A}) = \frac{m_e^2 R}{16\pi^2} \int e^{iqr} \left[ \frac{3\bar{A}^2 + 9\bar{A}q + 8q^2}{q^3(q + \bar{A})^3} \right] \times \left( \frac{\Lambda^2}{q^2 + \Lambda^2} \right)^4 d^3 q, \quad (7)$$

with  $g_V = 1.0$ ,  $g_A = 1.254$ ,  $f_W = \mu_p - \mu_n = 4.70$  [54], and  $\Lambda = 0.850$  GeV. Further, the central part of the recoil term is only retained in  $H_R(r, \bar{A})$  following Hirsch *et al.* [16]. The nuclear radius is taken to be  $R = R_0 A^{1/3}$  with  $R_0 = 1.2$  fm. The average energy of the nuclear intermediate states is  $\bar{A} = 1.12 A^{1/2}$  MeV [55].

The model-specific uncertainties associated with the NTMEs  $M_\alpha^{(\chi)}$  for the  $(\beta^- \beta^- \chi)_{0\nu}$  decay modes are evaluated statistically by estimating the mean and standard deviation of a set of 12 NTMEs, calculated in the PHFB approach [37] with the consideration of four different parametrizations of the effective two-body interaction and three different parametrizations of the SRC. The details about the four different parametrizations of the effective two-body interaction have already been given in Refs. [37–39]. By considering a form of Jastrow short-range correlations given in Ref. [21], the three different parametrizations of the SRC for the Miller-Spencer parametrization, Argonne  $NN$ , and CD-Bonn potentials, are denoted by SRC1, SRC2, and SRC3, respectively.

## III. RESULTS AND DISCUSSIONS

In the present work, the NTMEs  $M_{CR}^{(\chi)}$  and  $M_{\omega^2}^{(\chi)}$  are calculated employing the same wave functions as those used in Refs. [37–39]. The reliability of the wave functions has already been discussed in Ref. [37]. To exhibit the role of the

TABLE II. NTMEs  $M_{m_v}^{(\chi)}$ ,  $M_{\text{CR}}^{(\chi)}$ , and  $M_{\omega^2}^{(\chi)}$  for the Majoron-accompanied  $(\beta^- \beta^- \chi)_{0\nu}$  decay of  $^{100}\text{Mo}$  for the  $PQQ1$  parametrization.

NTMEs	Point	FNS	FNS + SRC			FNS + SRC( $\bar{A}/2$ )		
			SRC1	SRC2	SRC3	SRC1	SRC2	SRC3
$ M_{m_v}^{(\chi)} $	8.594	6.830	5.872	6.739	7.016	6.471	7.386	7.674
$M_{\text{CR}}^{(\chi)}$	-0.307	-0.264	-0.229	-0.263	-0.273	-0.259	-0.296	-0.306
$M_{F\omega^2}^{(\chi)} \times 10^3$	1.179	1.177	1.136	1.192	1.204	2.159	2.265	2.286
$M_{GT\omega^2}^{(\chi)} \times 10^3$	-5.800	-5.792	-5.596	-5.857	-5.911	-10.659	-11.149	-11.250
$ M_{\omega^2}^{(\chi)}  \times 10^3$	6.979	6.969	6.732	7.050	7.115	12.819	13.415	13.536

FNS and the SRC explicitly, the NTMEs  $M_{\text{CR}}^{(\chi)}$  and  $M_{\omega^2}^{(\chi)}$  for  $^{100}\text{Mo}$  calculated with the  $PQQ1$  parametrization within the approximations of point nucleons (P), nucleons having finite size (FNS), and FNS and SRC (FNS + SRC) are displayed in Table II. In addition, the NTME  $M_{m_v}^{(\chi)}$  [38] is also displayed for comparison. The NTME  $M_{m_v-VV}^{(\chi)} + M_{m_v-AA}^{(\chi)}$  has been taken as the point nucleon approximation of the NTME  $M_{m_v}^{(\chi)}$ . In the case of FNS + SRC, the NTMEs  $M_{m_v}^{(\chi)}$ ,  $M_{\text{CR}}^{(\chi)}$ , and  $M_{\omega^2}^{(\chi)}$  are also displayed with  $\bar{A}/2$  in the energy denominator to check the role of average denominator  $\bar{A}$ , in the present work.

It is noteworthy that the qualitative dependence of different neutrino potentials on momentum transfer  $q$  is of a different nature, and in contrast to the neutrino potential  $H_R(r, \bar{A})$ , the  $H_{\omega^2}(r, \bar{A})$  is quite singular in nature. The contributions from low-momentum  $q$  are crucial in the evolution of  $M_{\omega^2}^{(\chi)}$ , and as a result, the reliability of the calculated NTMEs is questionable. In fact, it turns out that the magnitudes of  $M_{\omega^2}^{(\chi)}$  are numerically uncertain by about 1 order magnitude, in accordance with Ref. [16].

### A. Effects due to FNS, SRC, and deformation of nuclei

The role of the FNS as well as the SRC can be displayed in the best possible way by plotting the radial evolution of NTMEs  $M_{m_v}^{(\chi)}$ ,  $M_{\text{CR}}^{(\chi)}$ , and  $M_{\omega^2}^{(\chi)}$  defined by  $M_{\alpha}^{(\chi)} = \int C_{\alpha}^{(\chi)}(r) dr$  [50]. In Fig. 1, the radial variations of  $C_{\text{CR}}^{(\chi)}$  and  $C_{\omega^2}^{(\chi)}$  for the  $^{100}\text{Mo}$  nucleus are displayed with the  $PQQ1$  parametrization of the effective two-body interaction in four cases, namely, FNS, FNS + SRC1, FNS + SRC2, and FNS + SRC3. The plot of the radial dependence of  $C_{\alpha}^{(\chi)}$  for  $^{96}\text{Zr}$ ,  $^{100}\text{Mo}$ ,  $^{128,130}\text{Te}$ , and  $^{150}\text{Nd}$  isotopes with the same four combination of FNS and SRC show that the distributions are peaked at the same position and, as an example, the radial variations of  $C_{\text{CR}}^{(\chi)}$  and  $C_{\omega^2}^{(\chi)}$  for SRC1 are shown in Fig. 2.

It can be noticed that the distribution of  $C_{\text{CR}}^{(\chi)}$  is peaked at  $r = 1.0$  fm for the FNS and the addition of SRC1 shifts the peak to 1.4 fm. However, the position of the peak is changed to  $r = 1.2$  fm with the inclusion of SRC2 and SRC3. Although, the radial distributions of  $C_{\text{CR}}^{(\chi)}$  extend up to about 10 fm, the maximum contribution to the radial evolution of  $M_{\text{CR}}^{(\chi)}$  results from the distribution of  $C_{\text{CR}}^{(\chi)}$  up to 3 fm. However, the distributions  $C_{\omega^2}^{(\chi)}$  are completely of a different nature, and in all four cases, the peak positions are at 1.4 fm. Further,

the distributions are oscillating in nature with decreasing amplitudes and the first peak is similar to the distributions of NTMEs  $M_{m_v}^{(\chi)}$  and  $M_{\text{CR}}^{(\chi)}$ . The distributions up to 15 fm contribute to the total matrix element  $M_{\omega^2}^{(\chi)}$ . With the other three parametrizations of the effective two-body interaction, the above observations also remain valid. The observed changes in NTMEs  $M_{\text{CR}}^{(\chi)}$  and  $M_{\omega^2}^{(\chi)}$  due to the FNS and the SRC are intimately related with the variations in the areas of curves under different cases.

In Table III, the effects due to the inclusion of FNS and FNS + SRC are analyzed in terms of the relative changes in the NTMEs  $M_{\alpha}^{(\chi)}$  (in %) for a given set of parametrizations of the effective two-body interaction. The relative changes under FNS and HOC/FNS + SRC are changes in corresponding NTMEs with respect to the point nucleon and FNS cases, respectively. Depending on the magnitude of form factor  $\Lambda$ ,

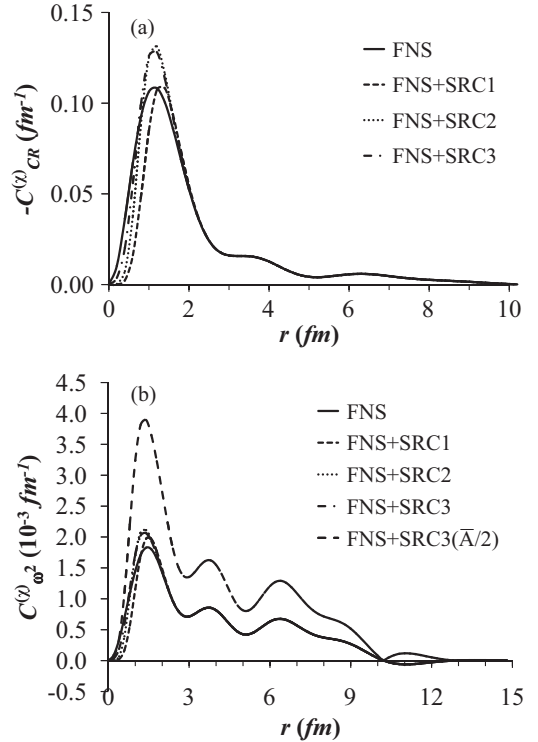


FIG. 1. Radial dependence of (a)  $C_{\text{CR}}^{(\chi)}(r)$  and (b)  $C_{\omega^2}^{(\chi)}(r)$  for the  $(\beta^- \beta^- \chi)_{0\nu}$  decay of the  $^{100}\text{Mo}$  isotope.

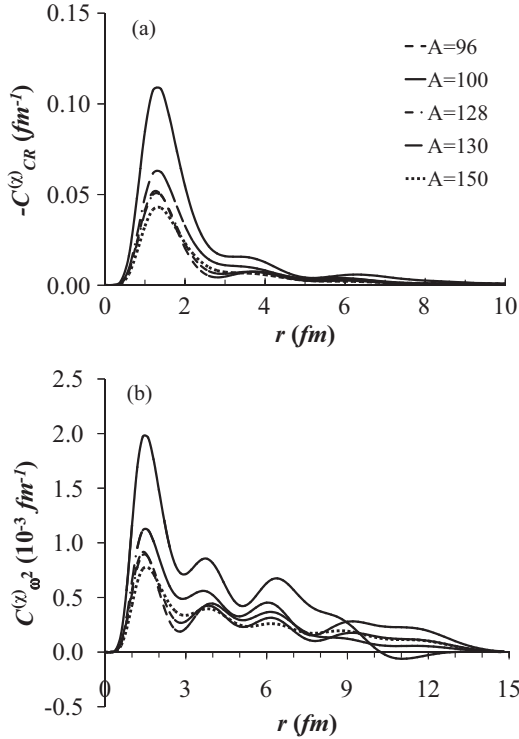


FIG. 2. Radial dependence of (a)  $C_{CR}^{(\chi)}(r)$  and (b)  $C_{\omega^2}^{(\chi)}(r)$  for the  $(\beta^- \beta^- \chi)_{0\nu}$  decay of  $^{96}\text{Zr}$ ,  $^{100}\text{Mo}$ ,  $^{128,130}\text{Te}$ , and  $^{150}\text{Nd}$  isotopes corresponding to the case FNS + SRC1.

the maximum change in the values of  $M_{m_v}^{(\chi)}$  and  $M_{CR}^{(\chi)}$  are between 11% and 16%, respectively. The NTMEs  $M_{m_v}^{(\chi)}$  are further reduced by 13.0% with the inclusion of HOC. With the addition of SRC, the NTMEs  $M_{m_v}^{(\chi)}$  and  $M_{CR}^{(\chi)}$  change by about 12%–16%, less than 2% and 2%–4% due to SRC1, SRC2, and SRC3, respectively. It is worth noting that the NTME  $M_{\omega^2}^{(\chi)}$  exhibits negligible change due to the FNS and the SRC.

TABLE III. Relative changes (in %) of the NTMEs  $M_{m_v}^{(\chi)}$ ,  $M_{CR}^{(\chi)}$  and  $M_{\omega^2}^{(\chi)}$  for the four different parametrizations of the effective two-body interaction, namely, (a)  $PQQ1$ , (b)  $PQQH1$ , (c)  $PQQ2$ , and (d)  $PQQH2$  with the inclusion of FNS, FNS + SRC (FNS + SRC1, FNS + SRC2, and FNS + SRC3), and average energy denominator  $\bar{A}/2$ .

NTMEs	FNS	HOC	FNS + SRC( $\bar{A}$ )			FNS + SRC( $\bar{A}/2$ )	
			FNS + SRC1	FNS + SRC2	FNS + SRC3		
$M_{m_v}^{(\chi)}$	(a)	8.94–10.63	11.17–12.96	12.38–15.61	0.99–1.96	2.48–2.97	9.22–12.64
	(b)	9.40–11.07	11.43–13.02	13.17–16.40	1.11–2.11	2.50–3.04	8.74–12.25
	(c)	8.95–10.68	10.13–13.00	12.40–15.71	0.99–1.99	2.39–2.99	9.19–12.62
	(d)	9.25–11.15	11.38–12.73	12.91–16.56	1.07–2.15	2.51–3.06	8.67–12.36
$M_{CR}^{(\chi)}$	(a)	13.12–15.13	–	11.88–14.71	0.10–0.22	3.13–3.70	11.82–16.26
	(b)	13.67–15.73	–	12.50–15.09	0.16–0.97	3.16–3.71	11.61–15.98
	(c)	12.55–15.19	–	11.51–14.79	0.10–0.93	2.98–3.71	11.78–16.23
	(d)	13.49–15.56	–	12.3–15.23	0.13–1.00	3.17–3.73	11.54–16.04
$M_{\omega^2}^{(\chi)}$	(a)	0.12–0.15	–	2.38–3.71	0.89–1.36	1.58–2.38	90.24–91.53
	(b)	0.13–0.18	–	2.72–4.39	1.02–1.56	1.79–2.76	89.90–91.40
	(c)	0.11–0.16	–	2.39–3.74	0.85–1.37	1.55–2.40	90.22–91.52
	(d)	0.13–0.18	–	2.61–4.49	1.01–1.59	1.73–2.83	89.85–91.44

By using the energy denominator  $\bar{A}/2$  instead of  $\bar{A}$ , the relative changes in NTME  $M_{CR}^{(\chi)}$  are similar to those found in  $M_{m_v}^{(\chi)}$ , which is at most 13.0%, supporting the employment of the closure approximation. However, the NTME  $M_{\omega^2}^{(\chi)}$  (also  $M_{F\omega^2}^{(\chi)}$  and  $M_{GT\omega^2}^{(\chi)}$ ) change appreciably as the  $\bar{A}$  is reduced by a factor of 2. The observed sensitivity of different NTMEs on the magnitude  $\bar{A}$  can be traced back to the structure of the neutrino potentials associated with different matrix elements. Taking the  $PQQ1$  parametrization as reference, the NTMEs  $M_{m_v}^{(\chi)}$  and  $M_{CR}^{(\chi)}$  change up to 25% with the consideration of the other three parametrizations, while the NTME  $M_{\omega^2}^{(\chi)}$  changes up to 34%.

By defining the deformation ratio  $D_\alpha^{(\chi)}$  as the ratio of  $M_\alpha^{(\chi)}$  at zero deformation ( $\zeta_{qq} = 0$ ) and  $M_\alpha^{(\chi)}$  at full deformation ( $\zeta_{qq} = 1$ ) [56], the effect of deformation on  $M_\alpha^{(\chi)}$  is quantified. It is observed that independent of the underlying mechanisms, the NTME  $M_\alpha^{(\chi)}$  is suppressed by a factor of about 2–6 due to deformation effects in the mass range  $A = 90–150$ . Thus, the deformation plays a crucial role in all the underlying mechanisms of the  $(\beta^- \beta^- \chi)_{0\nu}$  decay so far as the nuclear structure aspect is concerned.

## B. Uncertainties in nuclear transition matrix elements

The estimated averages  $\bar{M}_{CR}^{(\chi)}$  and  $\bar{M}_{\omega^2}^{(\chi)}$  with their respective variances  $\Delta \bar{M}_{CR}^{(\chi)}$  and  $\Delta \bar{M}_{\omega^2}^{(\chi)}$  for  $^{94,96}\text{Zr}$ ,  $^{100}\text{Mo}$ ,  $^{128,130}\text{Te}$ , and  $^{150}\text{Nd}$  isotopes are presented in Table IV. These are calculated by employing sets of 12 NTMEs obtained within the PHFB approach with the consideration of four different parametrizations of pairing plus multipolar type of effective two-body interaction and three different parametrizations of the SRC for both bare  $g_A = 1.254$  and quenched  $g_A = 1.0$  values of the axial vector coupling constant  $g_A$ . In addition, we also present the  $\bar{M}_{m_v}^{(\chi)}$  and  $\Delta \bar{M}_{m_v}^{(\chi)}$  of 12 NTMEs given in columns 4–6 of Table II of Ref. [38]. By considering NTMEs without (with) SRC1, the estimated uncertainties

TABLE IV. Average values for NTME  $\overline{M}_K^{(\chi)}$  and uncertainty  $\Delta \overline{M}_K^{(\chi)}$  for the  $(\beta^- \beta^- \chi)_{0\nu}$  decay of  $^{94,96}\text{Zr}$ ,  $^{100}\text{Mo}$ ,  $^{128,130}\text{Te}$ , and  $^{150}\text{Nd}$  isotopes. Both bare and quenched values of  $g_A$  are considered. Case I and Case II denote calculations with and without SRC1, respectively.

Nuclei	$g_A$	$\overline{M}_{m_\nu}^{(\chi)}$		$\overline{M}_{\text{CR}}^{(\chi)}$		$\overline{M}_{\text{CR}}^{(\chi)}$ [16]	$M_{\omega^2}^{(\chi)} \times 10^3$		$M_{\omega^2}^{(\chi)} \times 10^{3\pm 1}$ [16]
		Case I	Case II	Case I	Case II		Case I	Case II	
$^{94}\text{Zr}$	1.254	$3.873 \pm 0.373$	$4.071 \pm 0.246$	$0.158 \pm 0.015$	$0.165 \pm 0.010$	[16]	$4.429 \pm 0.560$	$4.500 \pm 0.562$	$\sim 1.0$
	1.0	$4.322 \pm 0.421$	$4.550 \pm 0.270$	$0.198 \pm 0.018$	$0.207 \pm 0.012$		$4.782 \pm 0.557$	$4.860 \pm 0.557$	
$^{96}\text{Zr}$	1.254	$2.857 \pm 0.264$	$3.021 \pm 0.119$	$0.115 \pm 0.010$	$0.121 \pm 0.004$	[16]	$3.198 \pm 0.240$	$3.256 \pm 0.229$	$\sim 1.0$
	1.0	$3.204 \pm 0.307$	$3.393 \pm 0.141$	$0.144 \pm 0.013$	$0.152 \pm 0.006$		$3.414 \pm 0.299$	$3.478 \pm 0.290$	
$^{100}\text{Mo}$	1.254	$6.250 \pm 0.638$	$6.575 \pm 0.452$	$0.246 \pm 0.024$	$0.258 \pm 0.016$	[16]	$6.386 \pm 0.709$	$6.499 \pm 0.711$	$\sim 1.0$
	1.0	$7.035 \pm 0.746$	$7.410 \pm 0.538$	$0.308 \pm 0.029$	$0.324 \pm 0.020$		$6.923 \pm 0.851$	$7.047 \pm 0.856$	
$^{128}\text{Te}$	1.254	$3.612 \pm 0.395$	$3.810 \pm 0.286$	$0.130 \pm 0.014$	$0.137 \pm 0.010$	[16]	$3.732 \pm 0.456$	$3.795 \pm 0.457$	$\sim 1.0$
	1.0	$4.088 \pm 0.450$	$4.316 \pm 0.321$	$0.163 \pm 0.018$	$0.172 \pm 0.013$		$4.161 \pm 0.518$	$4.230 \pm 0.519$	
$^{130}\text{Te}$	1.254	$4.046 \pm 0.497$	$4.254 \pm 0.406$	$0.143 \pm 0.016$	$0.151 \pm 0.012$	[16]	$4.330 \pm 0.892$	$4.395 \pm 0.908$	$\sim 1.0$
	1.0	$4.569 \pm 0.568$	$4.808 \pm 0.461$	$0.180 \pm 0.020$	$0.189 \pm 0.016$		$4.819 \pm 1.003$	$4.890 \pm 1.021$	
$^{150}\text{Nd}$	1.254	$2.826 \pm 0.430$	$2.957 \pm 0.408$	$0.094 \pm 0.014$	$0.099 \pm 0.013$	[16]	$3.042 \pm 0.496$	$3.081 \pm 0.508$	$\sim 1.0$
	1.0	$3.193 \pm 0.492$	$3.345 \pm 0.466$	$0.118 \pm 0.017$	$0.124 \pm 0.016$		$3.332 \pm 0.572$	$3.375 \pm 0.586$	

$\Delta \overline{M}_{\text{CR}}^{(\chi)}$  in  $\overline{M}_{\text{CR}}^{(\chi)}$  turn out to be about 4%–13% (8%–15%) to be compared with the uncertainties  $\Delta \overline{M}_{m_\nu}^{(\chi)}$  in  $\overline{M}_{m_\nu}^{(\chi)}$ , which are about 4%–14% (9%–15%). The uncertainties in both the NTMEs  $M_{m_\nu}^{(\chi)}$  and  $M_{\text{CR}}^{(\chi)}$  are of the same order, reflecting that the corresponding operators are of identical form. In addition, the statistically estimated theoretical uncertainties  $\Delta \overline{M}_{\omega^2}^{(\chi)}$  in NTME  $\overline{M}_{\omega^2}^{(\chi)}$  turn out to be 7.0%–21% (7.5%–21%) without (with) SRC1, exhibiting a negligible dependence on the SRC. In Table IV, we also present the NTMEs  $\overline{M}_{\text{CR}}^{(\chi)}$  and  $\overline{M}_{\omega^2}^{(\chi)}$  calculated by Hirsch *et al.* [16] within the *pn*-QRPA by employing the *G* matrix of the Paris potential for comparison. The maximum difference between the NTMEs calculated within the PHFB and *pn*-QRPA approaches is about a factor of 2. However, the impact of this difference on the total half-life  $T_{1/2}^{(0\nu\chi)}$  is not of much importance so far as conclusions of the present work are concerned.

### C. Nuclear sensitivities and limits on effective Majoron-neutrino couplings

Recently, the phase-space factors  $G_\alpha^{(\chi)}$  for the  $0^+ \rightarrow 0^+$  transition have been calculated by Kotila *et al.* [57] with  $g_A = 1.269$ . In the present work, we rescale them for  $g_A = 1.254$  and the phase-space factors for  $^{94}\text{Zr}$  are calculated following Hirsch *et al.* [16]. There is a large difference in the phase-space factors within classical and new Majoron models. In Table V, we present the nuclear sensitivities, which are related to sensitivities of Majoron-neutrino couplings  $\langle g_\alpha \rangle$ , defined by [58]

$$\xi^{(\chi)} = 10^{10} \sqrt{G_\alpha^{(\chi)}} |M_\alpha^{(\chi)}|, \quad (8)$$

with an arbitrary normalization factor  $10^{10}$  so that the nuclear sensitivities for the  $(\beta^- \beta^- \phi\phi)_{0\nu}$  decay modes are of order one. It can be noticed that the nuclear sensitivities for the  $(\beta^- \beta^- \chi)_{0\nu}$  decay of  $^{150}\text{Nd}$ ,  $^{100}\text{Mo}$ ,  $^{96}\text{Zr}$ ,  $^{130}\text{Te}$ ,  $^{94}\text{Zr}$ , and  $^{128}\text{Te}$  isotopes are in decreasing order of their magnitudes. In addition, the nuclear sensitivities of the promising nuclei

for the classical Majoron models are larger than those of new Majoron models by about a factor of  $10^{3-4}$ .

In columns 7–10 of Table VI, the extracted limits on the effective Majoron-neutrino coupling constants  $\langle g_\alpha \rangle$  from the largest observed limits on half-lives  $T_{1/2}^{(0\nu\chi)}$  of  $^{94,96}\text{Zr}$ ,  $^{100}\text{Mo}$ ,  $^{128}\text{Te}$ ,  $^{130}\text{Te}$  and  $^{150}\text{Nd}$  isotopes are displayed. The most stringent extracted limit on  $\langle g_\alpha \rangle < (2.00 - 2.79) \times 10^{-5}$  is obtained for  $^{100}\text{Mo}$  within classical Majoron models. Due to smaller NTMEs and phase-space factors, the same limits  $\langle g_\alpha \rangle$  within new Majoron models are larger than those of classical Majoron models by a factor of  $10^{4-5}$ . Because the sensitivities of the ongoing double- $\beta$ -decay experiments to the new Majoron models are quite weak, a comparison of the expected half-lives  $T_{1/2}^{(0\nu\chi)}$  within classical and new Majoron models is of experimental interest. In Table VII, the predicted half-lives  $T_{1/2}^{(0\nu\chi)}$  with  $\langle g_\alpha \rangle = 10^{-6}$  and  $g_A = 1.254$  ( $g_A = 1.0$ ) are presented for spectral indices  $n = 1$  and 3 of  $(\beta^- \beta^- \phi)_{0\nu}$  and  $n = 3$  and 7 of  $(\beta^- \beta^- \phi\phi)_{0\nu}$  decay modes. The smallest and largest magnitudes of half-lives correspond to  $^{150}\text{Nd}$  and  $^{128}\text{Te}$  isotopes, respectively. It is quite clear that in the classical Majoron models, the half-lives  $T_{1/2}^{(0\nu\chi)}$  for the potential nuclei are within the reach of planned experiments and none of the new Majoron models can produce an observable decay rate in the near future.

TABLE V. Nuclear sensitivities for the  $(\beta^- \beta^- \phi)_{0\nu}$  and  $(\beta^- \beta^- \phi\phi)_{0\nu}$  decay modes in different Majoron models.

Nuclei	$\xi_\alpha^{(\chi)}(\beta\beta\phi)$		$\xi_\alpha^{(\chi)}(\beta\beta\phi\phi)$	
	$n = 1$	$n = 3$	$n = 3$	$n = 7$
$^{94}\text{Zr}$	$0.147 \times 10^3$	0.162	0.007	0.004
$^{96}\text{Zr}$	$1.429 \times 10^3$	3.918	0.170	0.579
$^{100}\text{Mo}$	$2.528 \times 10^3$	6.325	0.253	0.728
$^{128}\text{Te}$	$0.105 \times 10^3$	0.068	0.003	0.001
$^{130}\text{Te}$	$1.359 \times 10^3$	2.913	0.124	0.262
$^{150}\text{Nd}$	$2.589 \times 10^3$	7.124	0.310	1.124

TABLE VI. Experimental limits on half-lives  $T_{1/2}^{(0\nu\chi)}$  and extracted effective Majoron-neutrino coupling  $\langle g_\alpha \rangle$ , for the  $(\beta^-\beta^-\chi)_{0\nu}$  decay of  $^{96}\text{Zr}$ ,  $^{100}\text{Mo}$ ,  $^{128,130}\text{Te}$ , and  $^{150}\text{Nd}$  isotopes. Both (a) bare and (b) quenched values of  $g_A = 1.254$  and  $g_A = 1.0$ , respectively, are considered.

Nuclei	$T_{1/2}^{(0\nu\chi)}$			Ref.	$g_A$	$\langle g_\alpha \rangle$		$\langle g_\alpha \rangle$	
	$n = 1$	$n = 3$	$n = 7$			$n = 1$	$n = 3$	$n = 3$	$n = 7$
$^{94}\text{Zr}$	$2.3 \times 10^{18}$			[59]	(a)	$4.49 \times 10^{-2}$			
					(b)	$6.32 \times 10^{-2}$			
$^{96}\text{Zr}$	$1.9 \times 10^{21}$	$5.8 \times 10^{20}$	$1.1 \times 10^{20}$	[60]	(a)	$1.61 \times 10^{-4}$	0.106	1.56	1.28
					(b)	$2.25 \times 10^{-4}$	0.133	1.90	1.56
$^{100}\text{Mo}$	$3.9 \times 10^{22}$	$1.0 \times 10^{22}$	$7.0 \times 10^{19}$	[61,62]	(a)	$2.00 \times 10^{-5}$	0.016	0.63	1.28
					(b)	$2.79 \times 10^{-5}$	0.020	0.76	1.54
$^{128}\text{Te}$	$2.0 \times 10^{24}$	$2.0 \times 10^{24}$	$2.0 \times 10^{24}$	[63]	(a)	$6.75 \times 10^{-5}$	0.104	1.47	2.62
					(b)	$9.37 \times 10^{-5}$	0.130	1.75	3.11
$^{130}\text{Te}$	$1.6 \times 10^{22}$	$9.0 \times 10^{22}$		[64,65]	(a)	$5.82 \times 10^{-5}$	0.011	0.52	
					(b)	$8.09 \times 10^{-5}$	0.014	0.62	
$^{150}\text{Nd}$	$1.52 \times 10^{21}$	$2.2 \times 10^{20}$	$4.7 \times 10^{19}$	[66]	(a)	$9.91 \times 10^{-5}$	0.095	1.48	1.14
					(b)	$1.38 \times 10^{-4}$	0.119	1.77	1.37

#### IV. CONCLUSIONS

The Majoron-accompanied neutrinoless double- $\beta$  ( $\beta^-\beta^-\chi)_{0\nu}$  decay of  $^{94,96}\text{Zr}$ ,  $^{100}\text{Mo}$ ,  $^{128,130}\text{Te}$ , and  $^{150}\text{Nd}$  isotopes has been studied within mechanisms involving both classical and new Majoron models. Uncertainties in the NTMEs have been estimated by employing sets of twelve NTMEs  $M_{m_\nu}^{(\chi)}$ ,  $M_{\text{CR}}^{(\chi)}$ , and  $M_{\omega^2}^{(\chi)}$  calculated using the PHFB formalism. In contrast to  $M_{m_\nu}^{(\chi)}$  and  $M_{\text{CR}}^{(\chi)}$ , the NTMEs  $M_{\omega^2}^{(\chi)}$  are numerically uncertain by 1 order of magnitude due to the singular nature of the neutrino potential  $H_{\omega^2}$ . Reducing the energy denominator by half, the change in NTMEs  $M_{m_\nu}^{(\chi)}$  and  $M_{\text{CR}}^{(\chi)}$  is smaller than 16%, and the NTMEs  $M_{\omega^2}^{(\chi)}$  vary by a factor of 2. The effects due to the FNS and the SRC on  $M_{m_\nu}^{(\chi)}$  and  $M_{\text{CR}}^{(\chi)}$  are below 16% and are almost negligible on the magnitude of  $M_{\omega^2}^{(\chi)}$ . The effects due to the deformation are between factors of 2 and 6 for all the three types of NTMEs.

The calculated sensitivities  $\xi^{(\chi)}$  for new Majoron models are smaller by 3 to 4 orders of magnitude than those of classical Majoron models. Using the average NTMEs  $\bar{M}_\alpha^{(\chi)}$  calculated in the PHFB model, limits on the effective Majoron-neutrino coupling constants  $\langle g_\alpha \rangle$  were extracted from the available largest limits on experimental half-lives  $T_{1/2}^{(0\nu\chi)}$ . Within

classical Majoron models, the most stringent limit on the Majoron-neutrino coupling constant  $\langle g_\alpha \rangle$  turns out to be  $< 2.0 \times 10^{-5}$  corresponding to the observed half-life of the  $^{100}\text{Mo}$  isotope. The extracted effective Majoron-neutrino coupling constants  $\langle g_\alpha \rangle$  for new Majoron models are 3–4 orders of magnitude larger than those of classical Majoron models. Further, the ongoing double- $\beta$ -decay experiments have a weak sensitivity to the new Majoron models. The calculated half-lives  $T_{1/2}^{(0\nu\chi)}$  for  $\langle g \rangle = 10^{-6}$  suggest that although in the ongoing and planned  $\beta\beta$  experiments, the classical Majoron-accompanied  $(\beta^-\beta^-\phi)_{0\nu}$  decay might be observed, it would be very difficult to observe the Majoron accompanied  $(\beta^-\beta^-\chi)_{0\nu}$  decay within new Majoron models in the near future.

#### ACKNOWLEDGMENTS

We thank Dr. J. G. Hirsch, for going through the manuscript and providing valuable suggestions. This work is partially supported by SERB, India (Grant No. SERB/F/5139/2013-14), DST-SERB (Grant No. SB/S2/HEP-007/2013), the Council of Scientific and Industrial Research (CSIR), India (Sanction No. 03(1216)/12/EMR-II), and the Indo-Italian Collaboration DST-MAE project via Grant No. INT/Italy/P-7/2012 (ER).

TABLE VII. Predicted half-lives  $T_{1/2}^{(0\nu\chi)}$  for the  $(\beta^-\beta^-\chi)_{0\nu}$  decay of  $^{96}\text{Zr}$ ,  $^{100}\text{Mo}$ ,  $^{128,130}\text{Te}$ , and  $^{150}\text{Nd}$  isotopes. Lower and upper values correspond to bare and quenched values of  $g_A = 1.254$  and  $g_A = 1.0$ , respectively.

Nuclei	$T_{1/2}^{(0\nu\phi)}$ (yr)			$T_{1/2}^{(0\nu\phi\phi)}$ (yr)	
	$n = 1$	$n = 3$	$n = 7$	$n = 3$	$n = 7$
$^{94}\text{Zr}$	$(4.65\text{--}9.19) \times 10^{27}$	$(3.81\text{--}6.00) \times 10^{33}$		$(1.95\text{--}4.13) \times 10^{48}$	$(7.83\text{--}16.6) \times 10^{48}$
$^{96}\text{Zr}$	$(4.90\text{--}9.60) \times 10^{25}$	$(6.51\text{--}10.2) \times 10^{30}$		$(3.47\text{--}7.51) \times 10^{45}$	$(2.98\text{--}6.46) \times 10^{44}$
$^{100}\text{Mo}$	$(1.56\text{--}3.05) \times 10^{25}$	$(2.50\text{--}3.93) \times 10^{30}$		$(1.56\text{--}3.27) \times 10^{45}$	$(1.88\text{--}3.96) \times 10^{44}$
$^{128}\text{Te}$	$(9.10\text{--}17.5) \times 10^{27}$	$(2.15\text{--}3.38) \times 10^{34}$		$(9.36\text{--}18.6) \times 10^{48}$	$(9.36\text{--}18.6) \times 10^{49}$
$^{130}\text{Te}$	$(5.41\text{--}10.5) \times 10^{25}$	$(1.18\text{--}1.85) \times 10^{31}$		$(6.52\text{--}13.0) \times 10^{45}$	$(1.45\text{--}2.90) \times 10^{45}$
$^{150}\text{Nd}$	$(1.49\text{--}2.88) \times 10^{25}$	$(1.97\text{--}3.10) \times 10^{30}$		$(1.04\text{--}2.15) \times 10^{45}$	$(7.92\text{--}16.3) \times 10^{43}$

- [1] A. S. Barabash, in *Proceedings of the Sixteenth Lomonosov Conference on Elementary Particle Physics, Moscow, Russia, 22–28 August 2013* (World Scientific, Singapore, 2015), pp. 295–299.
- [2] A. Garfagnini, *Int. J. Mod. Phys. Conf. Ser.* **31**, 1460286 (2014).
- [3] W. Tornow, [arXiv:1412.0734](https://arxiv.org/abs/1412.0734).
- [4] J. D. Vergados, H. Ejiri, and F. Šimkovic, *Rep. Prog. Phys.* **75**, 106301 (2012).
- [5] K. Oliv *et al.*, *Chin. Phys. C* **38**:09001, 626 (2014).
- [6] Y. Chikashige, R. N. Mohapatra, and R. D. Peccei, *Phys. Rev. Lett.* **45**, 1926 (1980); *Phys. Lett. B* **98**, 265 (1981).
- [7] G. B. Gelmini and M. Roncadelli, *Phys. Lett. B* **99**, 411 (1981).
- [8] H. M. Georgi, S. L. Glashow, and S. Nussinov, *Nucl. Phys. B* **193**, 297 (1981).
- [9] C. S. Aulakh and R. N. Mohapatra, *Phys. Lett. B* **119**, 136 (1982).
- [10] C. P. Burgess and J. M. Cline, *Phys. Lett. B* **298**, 141 (1993); *Phys. Rev. D* **49**, 5925 (1994).
- [11] C. D. Carone, *Phys. Lett. B* **308**, 85 (1993).
- [12] P. Bamert, C. P. Burgess, and R. N. Mohapatra, *Nucl. Phys. B* **449**, 25 (1995).
- [13] G. S. Abrams *et al.*, *Phys. Rev. Lett.* **63**, 724 (1989).
- [14] M. C. Gonzalez-Garcia and Y. Nir, *Phys. Lett. B* **232**, 383 (1989).
- [15] A. S. Barabash, *Phys. At. Nucl.* **73**, 162 (2010); *Phys. Part. Nucl.* **42**, 613 (2011).
- [16] M. Hirsch, H. V. Klapdor-Kleingrothaus, S. G. Kovalenko, and H. Päs, *Phys. Lett. B* **372**, 8 (1996).
- [17] G. A. Miller and J. E. Spencer, *Ann. Phys. (NY)* **100**, 562 (1976).
- [18] H. F. Wu, H. Q. Song, T. T. S. Kuo, W. K. Cheng, and D. Strottman, *Phys. Lett. B* **162**, 227 (1985).
- [19] J. G. Hirsch, O. Castaños, and P. O. Hess, *Nucl. Phys. A* **582**, 124 (1995).
- [20] M. Kortelainen and J. Suhonen, *Phys. Rev. C* **76**, 024315 (2007); M. Kortelainen, O. Civitarese, J. Suhonen, and J. Toivanen, *Phys. Lett. B* **647**, 128 (2007).
- [21] F. Šimkovic, A. Faessler, H. Müther, V. Rodin, and M. Stauf, *Phys. Rev. C* **79**, 055501 (2009).
- [22] J. Menéndez, D. Gazit, and A. Schwenk, *Phys. Rev. Lett.* **107**, 062501 (2011).
- [23] J. Suhonen and O. Civitarese, *Phys. Lett. B* **725**, 153 (2013).
- [24] J. Engel, F. Šimkovic, and P. Vogel, *Phys. Rev. C* **89**, 064308 (2014).
- [25] J. Barea, J. Kotila, and F. Iachello, *Phys. Rev. C* **91**, 034304 (2015).
- [26] E. Caurier, J. Menéndez, F. Nowacki, and A. Poves, *Phys. Rev. Lett.* **100**, 052503 (2008); E. Caurier, F. Nowacki, and A. Poves, *Eur. Phys. J. A* **36**, 195 (2008).
- [27] M. Horoi and S. Stoica, *Phys. Rev. C* **81**, 024321 (2010).
- [28] M. Horoi and B. A. Brown, *Phys. Rev. Lett.* **110**, 222502 (2013).
- [29] P. Vogel and M. R. Zirnbauer, *Phys. Rev. Lett.* **57**, 3148 (1986).
- [30] O. Civitarese, A. Faessler, and T. Tomoda, *Phys. Lett. B* **194**, 11 (1987).
- [31] J. Suhonen and O. Civitarese, *Phys. Rep.* **300**, 123 (1998).
- [32] A. Faessler and F. Šimkovic, *J. Phys. G: Nucl. Part. Phys.* **24**, 2139 (1998).
- [33] A. Faessler, V. Rodin, and F. Šimkovic, *J. Phys. G: Nucl. Part. Phys.* **39**, 124006 (2012); D. L. Fang, A. Faessler, V. Rodin, and F. Šimkovic, *Phys. Rev. C* **83**, 034320 (2011); **82**, 051301(R) (2010).
- [34] M. T. Mustonen and J. Engel, *Phys. Rev. C* **87**, 064302 (2013).
- [35] F. Šimkovic, V. Rodin, A. Faessler, and P. Vogel, *Phys. Rev. C* **87**, 045501 (2013).
- [36] R. Chandra, K. Chaturvedi, P. K. Rath, P. K. Raina, and J. G. Hirsch, *Europhys. Lett.* **86**, 32001 (2009).
- [37] P. K. Rath, R. Chandra, K. Chaturvedi, P. K. Raina, and J. G. Hirsch, *Phys. Rev. C* **82**, 064310 (2010).
- [38] P. K. Rath, R. Chandra, K. Chaturvedi, P. Lohani, P. K. Raina, and J. G. Hirsch, *Phys. Rev. C* **88**, 064322 (2013).
- [39] P. K. Rath, R. Chandra, P. K. Raina, K. Chaturvedi, and J. G. Hirsch, *Phys. Rev. C* **85**, 014308 (2012).
- [40] J. Barea, J. Kotila, and F. Iachello, *Phys. Rev. C* **87**, 014315 (2013); F. Iachello, J. Barea, and J. Kotila, *AIP Conf. Proc.* **1417**, 62 (2011); F. Iachello and J. Barea, *Nucl. Phys. B, Proc. Suppl.* **217**, 5 (2011); J. Barea and F. Iachello, *Phys. Rev. C* **79**, 044301 (2009).
- [41] N. Yosida and F. Iachello, [arXiv:1301.7172](https://arxiv.org/abs/1301.7172) (to be published in *Prog. Theor. Exp. Phys.*).
- [42] T. R. Rodríguez and G. Martínez-Pinedo, *Phys. Rev. Lett.* **105**, 252503 (2010).
- [43] J. M. Yao, L. S. Song, K. Hagino, P. Ring, and J. Meng, [arXiv:1410.6326](https://arxiv.org/abs/1410.6326).
- [44] S. M. Bilenky and J. A. Grifols, *Phys. Lett. B* **550**, 154 (2002).
- [45] P. Vogel, in *Current Aspects of Neutrino Physics*, edited by D. O. Caldwell (Springer, Berlin, 2001), Chap. 8, p. 177; [arXiv:nucl-th/0005020](https://arxiv.org/abs/nucl-th/0005020).
- [46] John N. Bahcall, Hitoshi Murayama, and C. Peña-Garay, *Phys. Rev. D* **70**, 033012 (2004).
- [47] F. T. Avignone, III, G. S. King, III, and Yu. G. Zdesenko, *New J. Phys.* **7**, 6 (2005); F. T. Avignone, III, *Prog. Part. Nucl. Phys.* **57**, 170 (2006).
- [48] V. A. Rodin, A. Faessler, F. Šimkovic, and P. Vogel, *Nucl. Phys. A* **766**, 107 (2006); **793**, 213 (2007); *Phys. Rev. C* **68**, 044302 (2003).
- [49] J. Suhonen, *Phys. Lett. B* **607**, 87 (2005).
- [50] F. Šimkovic, A. Faessler, V. Rodin, P. Vogel, and J. Engel, *Phys. Rev. C* **77**, 045503 (2008).
- [51] J. Engel, *J. Phys. G: Nucl. Part. Phys.* **42**, 034017 (2015).
- [52] J. Dobaczewski, W. Nazarewicz, and P. Reinhard, *J. Phys. G: Nucl. Part. Phys.* **41**, 074001 (2015).
- [53] P. K. Rath, R. Chandra, K. Chaturvedi, P. Lohani, P. K. Raina, and J. G. Hirsch, *Phys. Rev. C* **87**, 014301 (2013).
- [54] C. Barbero, M. Cline, F. Kromptic, and D. Tadic, *Phys. Lett. B* **392**, 419 (1997).
- [55] W. C. Haxton and G. J. Stephenson, Jr., *Prog. Part. Nucl. Phys.* **12**, 409 (1984).
- [56] K. Chaturvedi, R. Chandra, P. K. Rath, P. K. Raina, and J. G. Hirsch, *Phys. Rev. C* **78**, 054302 (2008).
- [57] J. Kotila, J. Barea, and F. Iachello, *Phys. Rev. C* **91**, 064310 (2015).
- [58] F. Šimkovic, G. Pantelis, J. D. Vergados, and A. Faessler, *Phys. Rev. C* **60**, 055502 (1999).
- [59] R. Arnold *et al.*, *Nucl. Phys. A* **658**, 299 (1999).
- [60] J. Argyriades *et al.*, *Nucl. Phys. A* **847**, 168 (2010).
- [61] R. Arnold *et al.*, *Phys. Rev. D* **89**, 111101 (2014).
- [62] R. Arnold *et al.*, *Nucl. Phys. A* **765**, 483 (2006).
- [63] O. K. Manuel, *J. Phys. G: Nucl. Part. Phys.* **17**, S221 (1991).
- [64] R. Arnold *et al.*, *Phys. Rev. Lett.* **107**, 062504 (2011).
- [65] C. Arnaboldi *et al.*, *Phys. Lett. B* **557**, 167 (2003).
- [66] J. Argyriades *et al.*, *Phys. Rev. C* **80**, 032501(R) (2009).